Piconewton-millisencond force steps reveal the transition kinetics and mechanism of the double stranded DNA elongation

SUPPORTING MATERIAL

1. Influence of viscosity on the kinetics of the elongation-untwisting of the ds-DNA during the overstretching transition.

A. Drag produced on the trapped bead by the viscosity of the medium. The change in position of the trapped bead during the movement of the piezoelectric stage reliably measures the tension on the molecule only if it is not influenced by the drag due to the movement of the solution accompanying the movement of the stage. The drag on the bead is $F_\eta = 6\pi\eta RV$, where η is the viscosity of the solution (10^{-3} Pa s, at 25 °C), R is the radius of the bead (1.64 or 1.09 μm) and V is the translational velocity of the bead. Considering that the stiffness of the molecule is ~60 pN μm^{-1} and the stiffness of the trap is 150 pN μm^{-1}, a step of 2 pN complete in 2 ms implies a bead movement of ~40 nm at a velocity of ~20 μm s^{-1}. Consequently, for the bead with R = 1.09 μm, F_η attains a value of 0.5 pN and decays with a time constant of 0.5 ms (1/4 the risetime of the step).

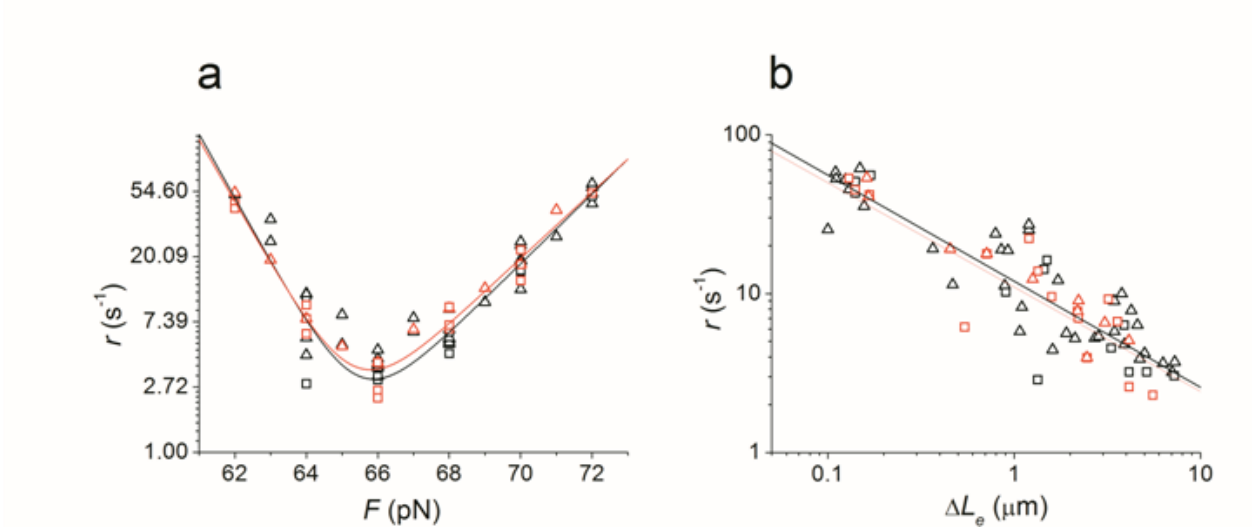

Fig. S1. (a): r - F relation for the 2 pN steps from Fig. 2d blue symbols. (b): r - ΔL relation for the 2 pN steps from the inset of Fig. 2c blue symbols. Red symbols refer to data obtained with 2.18 μm bead diameter (5 molecules); black symbols refer to data obtained with 3.28 μm bead diameter (12 molecules).

This analysis indicates that the viscous drag on the bead does not significantly influence the position of the bead during the step nor the observed elongation kinetics. A direct test of this conclusion is obtained by comparing the r-F relations obtained with different bead diameters. In Fig. S1a and S1b, the blue points data from in Fig. 2d and 2c (inset) respectively are unpooled to identify those obtained with beads of 3.28 μm diameter (black symbols, 12 molecules) and 2.18 μm

diameter (red symbols, 5 molecules). In this way it becomes evident the absence of any effect of the bead diameter on the overstretching kinetics. Eventually, it must be mentioned that the relaxation rate expected in the case of a translational damping process solely depends on the bead size which is constant during the entire experiment. It is therefore impossible that a convex profile of the *r-F* relation with rates spanning more than one order of magnitude is determined by translational drag

B. Rotational drag of the molecule while untwisting.

A rotational drag of the ds-DNA while untwisting in response to a rise in torque has been directly measured by attaching a bead near a nick and determining the angular velocity (1). In this way it has been shown that the untwisting takes several minutes and the drag dominates the elongation-untwisting velocity. However in that experiment the drag should be several time larger than in our experiment, as it is generated by the revolutions of a large bead accompanying the untwisting of the molecule.

During the overstretching transition under our conditions, the molecule of DNA elongates by 11 μm while it reduces the number of turns from 4500 to 1450, that is it untwists by 278 turns μm^{-1}. The largest elongation in response to a 2 pN step is ~5 μm attained within 0.5 s (Fig. 2). This implies a rotational speed ω of (278*5/0.5 =) 2780 turns s^{-1}, so that each of the two ends of the molecule should counter-rotate at 1390 turns s^{-1}. According to measurements of rotational drag in the experiment of Thomen et al. (2), where the two strands of DNA are attached to two independent beads and separated at different velocities, a torque of 0.6 k_BT would be necessary for the rotation at the speed of our overstretching transition. However, in Thomen et al. experiment the rotating stretch is at longitudinal force zero (and therefore the molecule is not straight), while during the overstretching transition the longitudinal force is ~65 pN and the molecule can be assimilated to a rigid rod. According to Levinthal & Crane (3) the rigid rod model leads to a torque $\vartheta = 4\pi\eta R_H^2 L_{eff}\ \omega$, where η is the viscosity of the solution as above, R_H the hydrodynamic radius of DNA (1.05 nm (2)) and L_{eff} the extension of the portion of DNA which rotates in order to release the torsional stress. The molecular extension in the middle of the plateau of the overstretching transition is approximately 22 μm which, under the assumption of torsional stress accumulating in the middle of the molecule, gives a L_{eff} of 11 μm. With ω = 1390 turns s^{-1} (= 8730 rad s^{-1}) the maximal frictional torque results to be 0.3 k_BT. If, however, the torsional stress is distributed uniformly along the whole length of the molecule, the resulting frictional torque should drop to 0.15 k_BT. A frictional reaction of 0.15-0.3 k_BT is expected to have a negligible effect on the kinetics of the B-S transition as demonstrated below.

The presence of an external torque (in this case of frictional origin) opposing the B-S transition not only modifies the free energy difference between S and B states but also the free-energy barriers that the system must overcome for the transition (see Fig. 3). The B-S barrier will be increased (transition more difficult) while the S-B barrier will be decreased (transition easier). Let's define x_B and x_S the distances between consecutive bps in the two states and θ_B and θ_S the twist angles between consecutive bps, with numerical values: x_B = 0.34 nm, x_S = 0.58 nm θ_B = 1/10 turns = 0.63 rad, θ_S = 1/30 turns = 0.21 rad. Assuming for simplicity that the transition state is in the middle between both x_S and x_B and θ_S and θ_B , the change in barrier height due to the presence of a viscous torque can be estimated and compared with the analogous change due to the presence of an external force. The maximum torque induced barrier change is $\Delta E_\tau = \tau\ (\theta_S - \theta_B.)/2 =$ 0.3 k_BT* 0.4/2 = 0.25 pN nm or 0.06 k_BT. while the barrier change caused by the external force F (~65 pN at the transition) is $\Delta E_F = F\ (x_S - x_B)/2$ = 65*0.24/2 = 7.8 pN nm or 1.9 k_BT. Thus, since the barrier change introduced by the viscous torque is smaller by a factor of 32 relative to the barrier change caused by the external force, the analysis presented in the text, which disregards this contribution, is correct.

A simple direct test of the influence of the rotational drag of the molecule on the kinetics of elongation is obtained by plotting the elongation rate r as a function of the length of the molecule L during the overstretching transition (Fig. S2). If the elongation kinetics was dominated by the viscous friction one would expect the relaxation rates to depend on L. Actually the r-L relation shows a U shaped dependence that is hardly compatible with the hypothesis that the rotational drag determines the elongation rate.

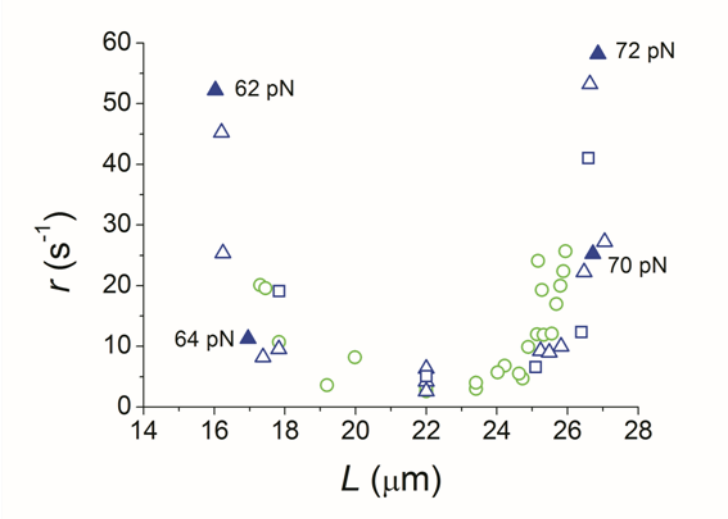

Fig. S2. Relation of the elongation rate (r) versus the molecular length (L) following 0.5 pN (green circles) and 2 pN (blue symbols) force steps. 2 pN data pooled from 13 molecules showing hysteresis in relaxation (triangles) and 4 molecules without hysteresis (squares). Data points are from the same experiments as Fig 2b. Figures close to filled symbols indicate the respective forces.

Another test is provided by the comparison of the rate of elongation in molecules that exhibit or not hysteresis (blue triangles and blue squares respectively in Fig. 2b-d). Assuming that the presence of nicks is revealed by the presence of hysteresis, it is expected that the length of independently rotating units during the overstretching transition is shorter for blue triangles than for blue squares. Consequently the finding that r is the same for the same force supports the idea that the rotational drag has not influence on the overstretching kinetics.

A further test is provided by the mechanical protocol described in the text, that allows to compare the responses to 2 and 0.5 pN force steps. For the same force, the extent of elongation (and thus ω) is smaller with the smaller step (see text). Since the rotational drag depends linearly on ω, if it was dominating the kinetics of the process, it would have generated a larger rate constant of elongation for the smaller step. However the observed rate constant is the same at the same force for either step size (Figs. 2b and 2d, blue 2 pN, green 0.5 pN). On the other hand, when the rate constant of elongation is plotted against the extent of elongation (Fig. 2c), the relation for 0.5 pN is shifted downward with respect to that for 2 pN, as predicted by the two state model (see Eq. S7 in the Supporting Material 2).

Both the theoretical treatment and the experimental evidences given above support the conclusion that the rate of DNA elongation following force steps applied in the overstretching transition region is mainly determined by the kinetics of the two state reaction. The conclusion is supported by the findings described in the text that: (*i*) r depends only on the force at the end of the step (Fig. 2b, d) and does not depends on neither the step size nor the length of the molecule, (*ii*) the slope of the log r – log ΔL_e relation (Fig. 2c inset) is -0.6, << 1, (see the Supporting Material 2)

2. Assessing the validity of the two state reaction assumption for the overstretching transition.

Here we verify that the two state reaction model proposed (see Fig. 3) is able to account both for the equilibrium and the relaxation kinetics of the overstretching transition.

The unidirectional transition rates between the two conformations k_+ and k_- depend on an additional parameters Ω, a kinetic pre-factor which is related to the viscous drag experienced by the molecule

in its motion along the reaction coordinate and to the shape of the molecular potential energy near the transition state. Thus, according to Kramers-Bells theory, the A_+ and A_- parameters are:

$$A_+ = \Omega \, e^{-\frac{\Delta G^{\ddagger}_+}{k_B T}} \qquad \text{Eq. S1}$$

and $A_- = \Omega\, e^{-\frac{\Delta G^{\ddagger}_+ - \Delta G}{k_B T}}$ Eq. S2.

The force (F_m) corresponding to the minimal relaxation rate *r(F)* is

$$F_m = \frac{\Delta G - k_B T \ln(x^{\ddagger}_+ / x^{\ddagger}_-)}{x^{\ddagger}_+ + x^{\ddagger}_-} = F_e - \frac{k_B T \ln(x^{\ddagger}_+ / x^{\ddagger}_-)}{x^{\ddagger}_+ + x^{\ddagger}_-}$$ Eq. S3,

where F_e is the coexistence force, the force at which the probabilities to reside in the compact and extended state (p_{cmp} and p_{ext}) are equal.

Also the equilibrium probabilities at each force are known:

$$p_{cmp}(F) = \frac{1}{1+\exp\left(-\frac{\Delta G - F(x^{\ddagger}_+ + x^{\ddagger}_-)}{k_B T}\right)}$$ Eq. S4

and $$p_{ext}(F) = \frac{\exp\left(-\frac{\Delta G - F(x^{\ddagger}_+ + x^{\ddagger}_-)}{k_B T}\right)}{1+\exp\left(-\frac{\Delta G - F(x^{\ddagger}_+ + x^{\ddagger}_-)}{k_B T}\right)}$$ Eq. S5.

$p_{ext}(F)$ grows monotonically with F, having maximal first derivative at the coexistence force, $F_e = \Delta G/(x^{\ddagger}_+ + x^{\ddagger}_-)$. At this force $\Delta G = F \cdot (x^{\ddagger}_+ + x^{\ddagger}_-)$, that is, the work done for the elongation equals the free energy difference between the compact and the extended state. We note that only for symmetric landscapes, $x^{\ddagger}_+ = x^{\ddagger}_-$, F_e coincides with F_m, the force of minimal relaxation rate.

During a positive staircase of force steps, when the force is changed from F to $F + \Delta F$ the probability to be in the extended state grows and, after equilibration, $N\,(p_{ext}(F+\Delta F) - p_{ext}(F))$ units have extended, where N is the total number of extensible units. It is therefore straightforward to compute the equilibrium force-extension profile which, according to the expressions for p_{ext} and p_{cmp}, only depends on the two parameters ΔG and $x_+ + x_-$. In Fig. S3 the experimental force-extension relation (black trace) from Fig. 1b' is compared to the theoretical relation (red dashed line) obtained with the ΔG and $x_+ + x_-$ chosen by fitting the elongation rates with the procedure described in the test. The agreement shows that the model developed to fit the observed relaxation kinetics is also capable of reproducing the equilibrium kinetics.

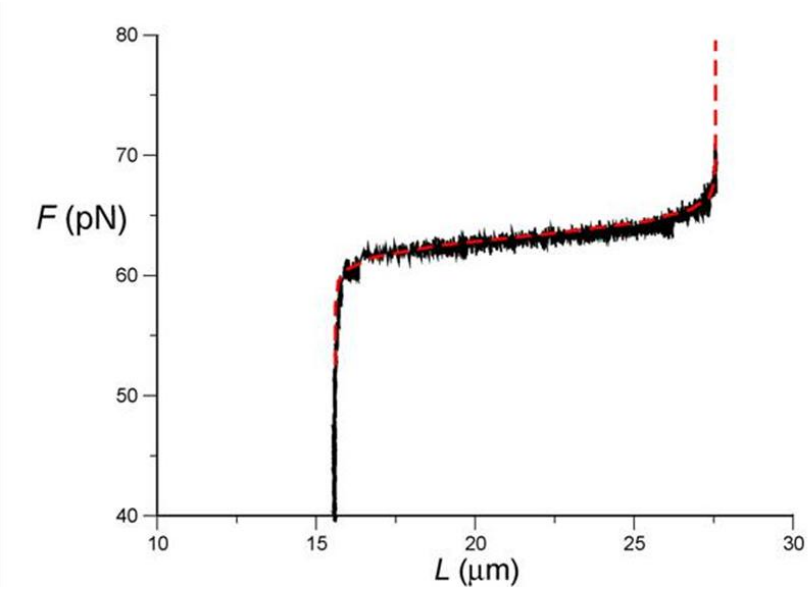

Fig. S3. Comparison between the experimental force-extension relation (black traces) and the theoretical relation (red trace) calculated with the p_{ext} and p_{cmp} equilibrium probabilities and the parameters ΔG and $x_+ + x_-$ obtained by fitting the elongation rates elicited by force steps. In order to reproduce the experimental curve the base pair separations of B and S state were set to 0.325 nm and 0.57 nm respectively.

The molecular elongation at force F is

$$\Delta L_e(F) \approx N\, \partial_F\, p_{ext}(F)\, \Delta F\, (x^{\ddagger}_{+} + x^{\ddagger}_{-}) \qquad \text{Eq. S6,}$$

where p_{ext} has been expanded to the first order. An expression for $r(\Delta L_e)$ can be obtained by inverting $\Delta L_e(F)$ and substituting into $r(F)$. $\Delta L_e(F)$, however, is a non monotonic function of F, growing before F_e and diminishing after. $F(\Delta L_e)$ has therefore two branches: $F_{\text{low}}(\Delta L_e)$ for $F<F_e$ and $F_{\text{high}}(\Delta L_e)$ for $F>F_e$. Substituting the two branches into $r(F)$ one gets two expressions for $r_{\text{low}}(\Delta L_e)$ and $r_{\text{high}}(\Delta L_e)$, which, after some algebra, can be shown to diverge in the low extension regime with exponents $x^{\ddagger}_{-}/(x^{\ddagger}_{+} + x^{\ddagger}_{-})$ and $x^{\ddagger}_{+}/(x^{\ddagger}_{+} + x^{\ddagger}_{-})$ respectively. More precisely

$$r_{low} \approx \Omega \left(\frac{4\Delta L_{TOT}\,(x^{\ddagger}_{+} + x^{\ddagger}_{-})\Delta F}{k_B T\ \Delta L_e} \right)^{\frac{x^{\ddagger}_{-}}{x^{\ddagger}_{+}+x^{\ddagger}_{-}}} \quad \text{and} \quad r_{high} \approx \Omega \left(\frac{4\Delta L_{TOT}\,(x^{\ddagger}_{+} + x^{\ddagger}_{-})\Delta F}{k_B T\ \Delta L_e} \right)^{\frac{x^{\ddagger}_{+}}{x^{\ddagger}_{+}+x^{\ddagger}_{-}}} \qquad \text{Eq.S7,}$$

where ΔL_{TOT} is the total elongation due to overstretching.

In our case using the values for $x^{\ddagger}_{-}$ and $x^{\ddagger}_{+}$ obtained by fitting the rate versus force relations , these two exponents amount to 0.4 and 0.6. In Fig. 2c of the text, the logarithmic plot of the rate versus elongation indicates that the exponent of the power equation is -0.6, the same as that expected for r_{high}-ΔL_e branch, to which the majority of the data refer. This suggests that, although some degree of interface propagation might be present in the elongation process, the cooperative elongation of

regions of DNA approximately 25 bp long represents the rate limiting step for the overstretching transition. The downward shift of the rate-versus-elongation profile following a decrease in ΔF as depicted in Fig. 2c also quantitatively agrees with Eq. S7 which predicts that, for the same elongation, rates should be proportional to $\Delta F^{x^{\ddagger}_{\pm}/(x^{\ddagger}_{+}+x^{\ddagger}_{-})}$. Note that Eq. S7 predicts also that a downward shift similar to that in Fig. 2c would be observed using 2 pN steps in a molecule ¼ the length of the whole DNA molecule. In fact, for the same elongation, rates should be proportional to $\Delta L_{TOT}^{x^{\ddagger}_{\pm}/(x^{\ddagger}_{+}+x^{\ddagger}_{-})}$, where ΔL_{TOT}, the total overstretching elongation, is a fixed fraction (0.7) of the length of the molecule.

3. Fitting the relation between rate of elongation and force with the four parameter equation.

The equation expressing the relation between the rate of elongation (r) and force (F) is:

$$r = k_{+} + k_{-} = A_{+} \exp\left(\frac{F\, x^{\ddagger}_{+}}{k_B T}\right) + A_{-} \exp\left(-\frac{F\, x^{\ddagger}_{-}}{k_B T}\right) \qquad \text{Eq. S8}$$

and is fitted to the r-F data on the entire force range for both force step sizes (purple line in Fig. 3d). The equation is a downward convex function of F with a minimum at $F_{\mathrm{m}} = \frac{k_B T \ln(A_{-} x^{\ddagger}_{-} / A_{+} x^{\ddagger}_{+})}{x^{\ddagger}_{+} + x^{\ddagger}_{-}}$. The values from the four parameters are: ln A_{+} = -34.12 ± 1.65, $x^{\ddagger}_{+}$ = 2.21 ± 0.11 nm, ln A_{-} = 59.19 ± 3.55; $x^{\ddagger}_{-}$ = 3.70 ± 0.23 nm (so that F_{m} = 65.81), and are almost identical to those determined by separately fitting the low and high force branch of the relations, assessing the validity of the assumption in the text that in the two sides of the overstretching transition the contribution of the minor term can be neglected.

4. Introducing heterogeneity in the model.

In the text we have assumed that DNA overstretches in discrete, cooperative units which are all characterized by the same size and the same free energy profile. Such assumptions are clearly an oversimplification since it is more sensible to expect that, whatever the microscopic mechanism generating the observed cooperativity, the sizes of the molecular regions undergoing cooperative overstretching will cover a continuous and somewhat extended range of sizes. We here test how the behavior of the proposed model is affected by the introduction of heterogeneity in the size of the cooperatively overstrecthing units .

Monte Carlo simulations analogous to that described in the text were performed for a set of 2200

two state units, each of 22 bps. In this set of simulations, however, a certain amount of eterogeneity was introduced in the structural and energetic parameters of the model which maintained on average the values obtained by fitting the experimental data. The system was integrated for 5 s. Fig. S4 shows that a stochastic variability of the 30% in x_+ and x_- does not significantly alter the profile of the transition at equilibrium.

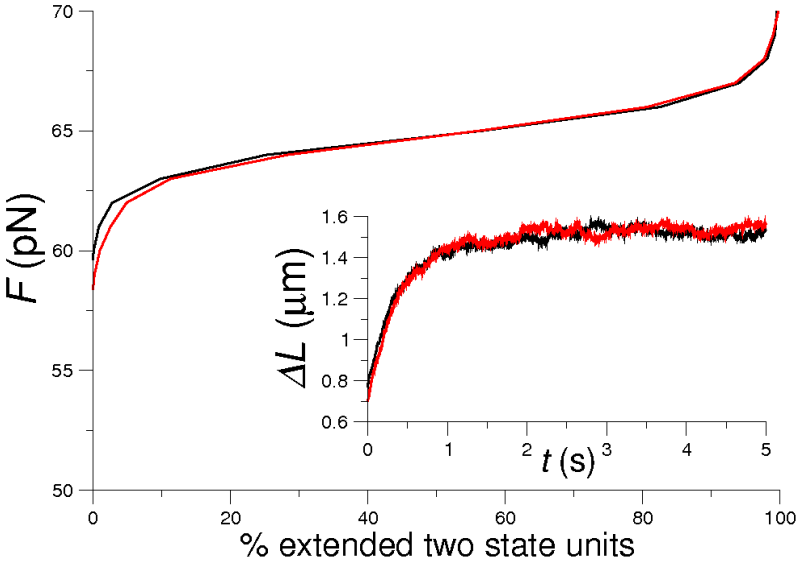

Fig. S4. Equilibrium force-extension relation of a system of 2200 two state units of identical size (black) and with 30% variation in size (red). The degree of extension is expressed as % of extended units. Inset: time course of elongation following 1 pN force step (intermediate between the 0.5 and 2 pN force steps of the experiments) to 65 pN; red and black as in the main frame.

The apparent cooperativity of the transition, assessed by means of a sigmoidal fit of the equilibrium profile, increases less than 10% as soon as the parameters $ln(A_+)$ and $ln(A_-)$ are chosen proportionally to x_+ and x_-. Also the elongation following a force step (see inset of Fig. S4 for the elongation at 65 pN) appears to satisfactorily reproduce the observed time course since, despite being in principle a sum of exponentials, it still fits a single exponential (dashed line). Notably even the noise in the calculated trace is similar to the observed one (±1 μm).

In the previous analysis we have varied both the relevant energetic parameters - the free energy barrier $\Delta G^{\ddagger}_{+}$ and the free energy difference between extended and compact state ΔG_- that dictate the relaxation rates of each cooperatively overstretching unit. By varying them independently one can get a feeling about the possible range the variability.

The introduction of heterogeneity in the free-energy barrier $\Delta G^{\ddagger}_{+}$ is not expected to change the equilibrium profile of the transition since the equilibrium probabilities p_{cmp} and p_{ext} only depend on ΔG, but it does change the relaxation kinetics. Fig. S5 shows that the introduction of a gaussian

variability in $\Delta G^{\ddagger}_{+}$ with standard deviation of 10% produces an elongation time course which departs markedly from exponential. Although an exponential fit holds very similar results for simulations performed with a fixed and a variable free energy barrier, in this last case the time course is characterized by the presence of an early fast rising portion corresponding to the smallest barriers in the system. This feature is absent in the observed time courses (Fig. 2a), indicating that any variability in the value of the free energy barrier is lower than 10%.

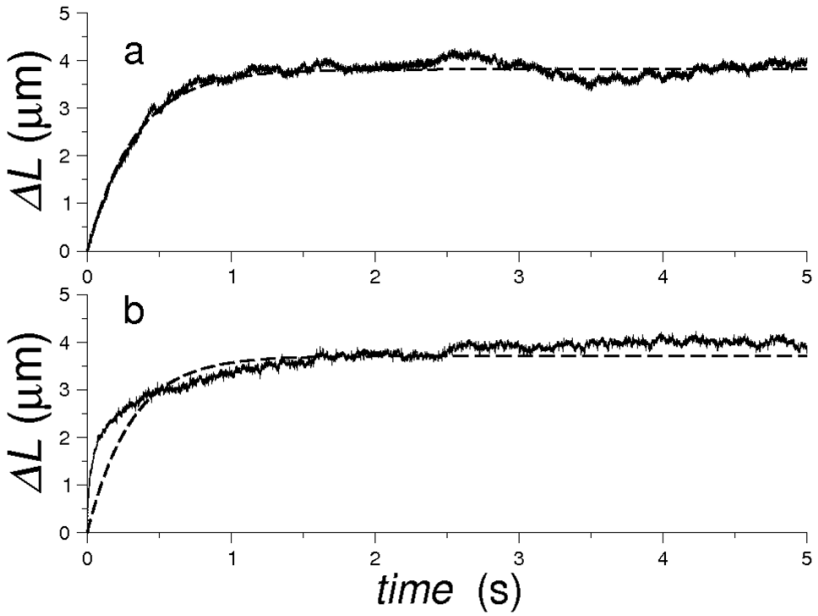

Fig. S5. Time course of an elongation following a 1 pN force step to 65 pN calculated for a system composed of identical two-state units (a) and for one with a 10% heterogeneity in $\Delta G^{\ddagger}_{+}$ (b). Dashed lines are single exponential fits.

As far as ΔG is concerned, a gaussian variability with standard deviation of 1% lowers the apparent cooperativity by only 10% (data not shown) without substantial effects on the elongation rate. Larger ΔG variabilities, however, quickly introduce slow components in the elongation time course, preventing from reaching equilibrium in the 5 s observation time. The fact that the experimental stretching curves are almost superposable to the release curves therefore suggests that also the variability on ΔG is lower than 10%.

In conclusion, by interpreting our experimental data with a two state model where all cooperatively overstretching units have the same length, we introduce only a small underestimate in the degree of cooperativity of the system. Moreover, the exponential character of the observed kinetic profiles and the good equilibration reached by the process in the 5 s time scale suggest that the heterogeneity in the energetic parameters is lower than 10%.

REFERENCES

1. Bryant, Z., M. D. Stone, J. Gore, S. B. Smith, N. R. Cozzarelli and C. Bustamante. 2003. Structural Transitions and Elasticity from Torque Measurements on DNA. Nature 424:338-341.

2. Thomen, P., U. Bockelmann and F. Heslot. 2002. Rotational Drag on DNA: A Single Molecule Experiment. Phys. Rev. Lett. 88:248102.

3. Levinthal, C. and H. R. Crane. 1956. On the Unwinding of DNA. Proc. Natl. Acad. Sci. USA 42:436-438.